

NJC

Accepted Manuscript

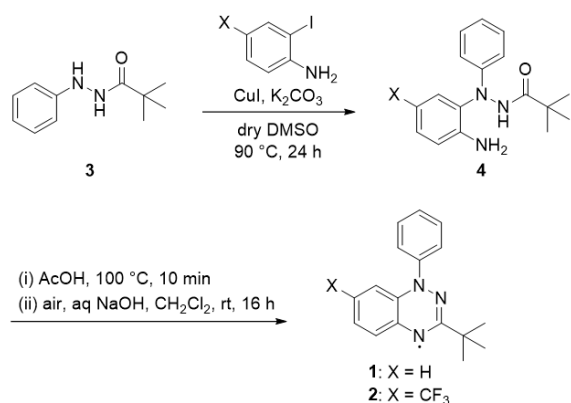


This is an *Accepted Manuscript*, which has been through the Royal Society of Chemistry peer review process and has been accepted for publication.

Accepted Manuscripts are published online shortly after acceptance, before technical editing, formatting and proof reading. Using this free service, authors can make their results available to the community, in citable form, before we publish the edited article. We will replace this *Accepted Manuscript* with the edited and formatted *Advance Article* as soon as it is available.

You can find more information about *Accepted Manuscripts* in the [Information for Authors](#).

Please note that technical editing may introduce minor changes to the text and/or graphics, which may alter content. The journal's standard [Terms & Conditions](#) and the [Ethical guidelines](#) still apply. In no event shall the Royal Society of Chemistry be held responsible for any errors or omissions in this *Accepted Manuscript* or any consequences arising from the use of any information it contains.



Scheme 1 Synthetic route of the benzotriazinyl radicals.

tuent effect on the magneto-structural correlation is discussed. The physicochemical properties of **1** are also reported.

Results and discussion

Preparation of benzotriazinyl radicals

Radical **2** was prepared according to Scheme 1. *N*'-phenyl-*N*-pivaloylhydrazine **3** was obtained by condensation between pivaloyl chloride and phenylhydrazine in CH₂Cl₂. A trifluoromethyl-substituted radical precursor **4** was formed using the Cu-catalyzed C-N coupling with the corresponding 2-iodoaniline, as reported by Ma and co-workers.²¹ Compound **4** was not purified due to its instability. The cyclization and oxidation under basic conditions of **4**, using a method similar to that of Koutentis and co-workers,¹⁸ afforded the trifluoromethyl-substituted radical **2** in 26% yield in 2 steps. The UV-Vis spectra of **1** and **2** are reported in the supporting information. Radical **1** was prepared in the same manner in 34% yield. The physical data of **1** are the same as in previous studies.^{19,20}

Single crystal X-ray crystallographic analysis

X-ray crystallographic analyses were performed with Mo *K* α radiation at 296 K. Single crystals of **1** and **2** suitable for an X-ray analysis were obtained by the slow evaporation of *n*-hexane and CH₃OH solutions, respectively. Radicals **1** and **2** belong to the monoclinic spacegroup *P*2₁/*n* and *C**c*, respectively. The ORTEP drawings of **1** and **2** are shown in Figure 2. The bond lengths of the amidrazonyl moiety for **1** ($d_{\text{N1-N2}} = 1.366(2)$ Å, $d_{\text{N2-C1}} = 1.337(2)$ Å, $d_{\text{C1-N3}} = 1.327(2)$ Å) indicate that an unpaired electron was delocalized over the heterocyclic ring. The dihedral angle between the *N*-phenyl group and amidrazonyl ring is 73.85(6)°, which is greater than that of Blatter's radical(54.0°)²² and its derivatives. This suggests that the steric effect of the *N*-phenyl group and *tert*-butyl group contribute to the stability of the radical. The bond lengths of the trifluoromethyl-substituted radical **2** ($d_{\text{N1-N2}} = 1.357(6)$ Å, $d_{\text{N2-C1}} = 1.338(7)$ Å, $d_{\text{C1-N3}} = 1.331(7)$ Å) are similar to those of radical **1**. The dihedral angle of **2** is 82.18(17)°, which is greater than that of **1** due to the molecular packing effect.

In the molecular packing of radical **1**, there is a head-to-head structure, which forms a 1D column structure along the *b* axis without a π - π interaction between the benzotriazinyl moieties (Figure 3). The heterocyclic ring appears not to have any contacts with other rings, which suggests a weak intermolecular magnetic interaction. This is consistent with a previous study, in which its magnetic susceptibility followed the Curie-Weiss law with the negative Weiss constant $\theta = -0.3$ K reported by Mukai and co-workers.²⁰ Radical **2** also formed a slipped 1D column structure along the *a* axis and there is a head-to-tail structure antiparallel along the *b* axis (Figure 4). In the 1D column, the distance between the benzotriazinyl rings is 4.35 Å because the bulky *tert*-butyl group prevents close contact of the π conjugation system.

According to the DFT calculation at the UB3LYP / 6-31G(d) level, the magnitudes of the dipole moments for **1** and **2** are

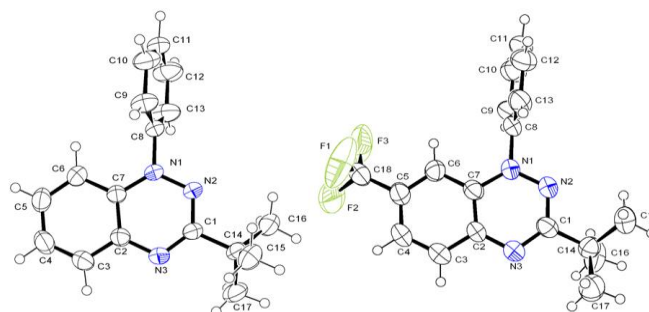


Figure 2 ORTEP drawings of **1**(left) and **2**(right). Thermal ellipsoids are shown as 50% probability.

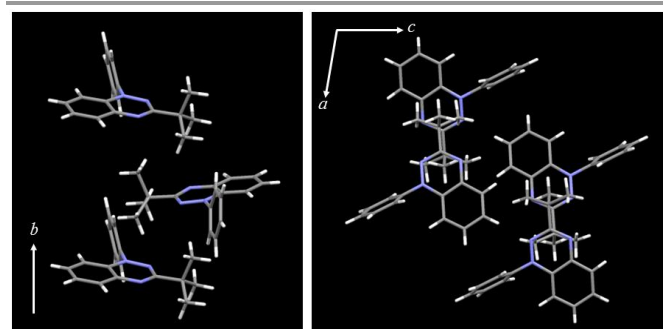


Figure 3 Crystal structure of **1** along *b* axis(left) and *b* axis projection(right).

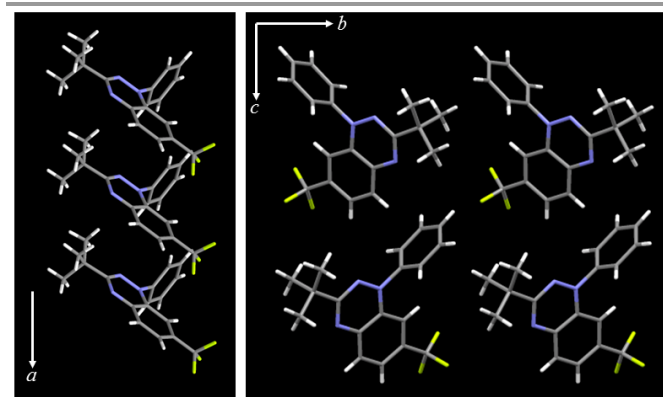


Figure 4 Crystal structure of **2** along *a* axis (left) and *a* axis projection (right).

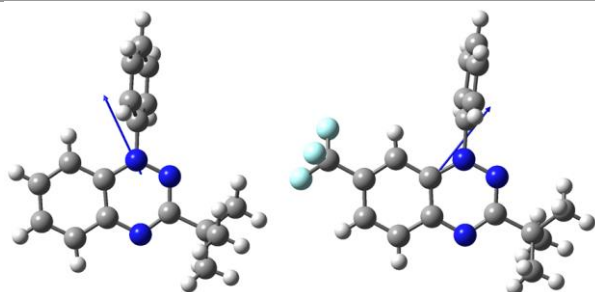


Figure 5 Calculated dipole moments of **1**(left) and **2**(right) at UB3LYP/6-31G(d) level.

3.29 D and 2.93 D, respectively (Figure 5). The moment of **2** decreased due to the trifluoromethyl group. In the crystal of **1**, the molecules cancel the moment in the column, however, the benzotriazinyl **2** is aligned in the same direction in the column and cancelled the moment between the columns along the *b* axis.

Magnetic property of radical **2**

The magnetic susceptibility measurement of the polycrystalline sample for **2** was carried out in the temperature range of 1.8–300 K. The temperature dependence of χ_m^{-1} and $\chi_m T$ are shown in Figure 6. The behavior of χ_m^{-1} followed the Curie-Weiss law, $\chi_m = C / (T - \theta)$, with $C = 0.369 \text{ emu K mol}^{-1}$ and $\theta = +0.7 \text{ K}$ above 50 K. The Curie constant was close to the expected $S = 1/2$ spin system. The presence of a ferromagnetic interaction was predicted due to the positive Weiss constant θ . This $\chi_m T$ value was almost constant above 40 K and gradually increased with the decreasing temperature. This suggests the existence of a ferromagnetic interaction between the benzotriazinyl radicals. The thermal behavior of the magnetic susceptibility can be analyzed using the Heisenberg 1D chain model (1). The behavior can be well described by the empirical equation (2) reported by Baker and co-workers²³ and the best-fit result is shown in Figure 6 as a solid line. The estimated magnitude of coupling with $J / k_B = +0.91 \text{ K}$ indicates that radical **2** formed a 1D ferromagnetic chain. This value is similar to that of **7TB** ($J / k_B = +1.49 \text{ K}$).¹⁷ An interchain antiferromagnetic interaction was observed at low temperature for **7TB**, however, the derivative **2** behaves as an ideal 1D ferromagnetic chain in the measured temperature range.

$$H = -J \sum_{i=1}^{n-1} S_i \times S_{i+1} \quad (1)$$

$$C_m = \frac{N_A g^2 m_B^2}{k_B T} F(J, T) \quad (2)$$

with

$$F(J, T) = \frac{1}{4} \frac{1 + 5.7979916x + 16.902653x^2 + 29.376885x^3 + 28.832959x^4 + 14.036918x^5}{1 + 2.7979916x + 7.008678x^2 + 8.6538644x^3 + 4.5743114x^4} x^{3/2}$$

and

$$x = \frac{J}{2k_B T}$$

To clarify the magnetic coupling, the magnetic field dependence of the magnetization was measured at 1.9 K

(Figure 6). The magnetization plots exceed the theoretical Brillouin curve for the $S = 1/2$ spin system and follows the $S = 1$ system. This indicates that a ferromagnetic interaction with $S = 1$ on average was dominant in the column.

DFT calculation and magneto-structural correlation

The single point calculation was carried out by the Gaussian 03W package²⁴ at the UB3LYP/6-31G(d) level using the crystal coordinate data. The singly occupied molecular orbital (SOMO) of **2** is shown in Figure 7. The SOMO of **2** was mainly distributed on the benzotriazinyl moiety and slightly delocalized over the CF_3 group. The computation suggests that the *N*-phenyl group is free from the π conjugation system due to the large dihedral angle against the amidrazonyl ring in the solid state. To understand the contribution of the ferromagnetic interaction in the 1D-column, the magnetic exchange parameter J was estimated using Yamaguchi's equation²⁵ (3)

$$J = \frac{E_{BS} - E_T}{\langle S^2 \rangle_T - \langle S^2 \rangle_{BS}} \quad (3)$$

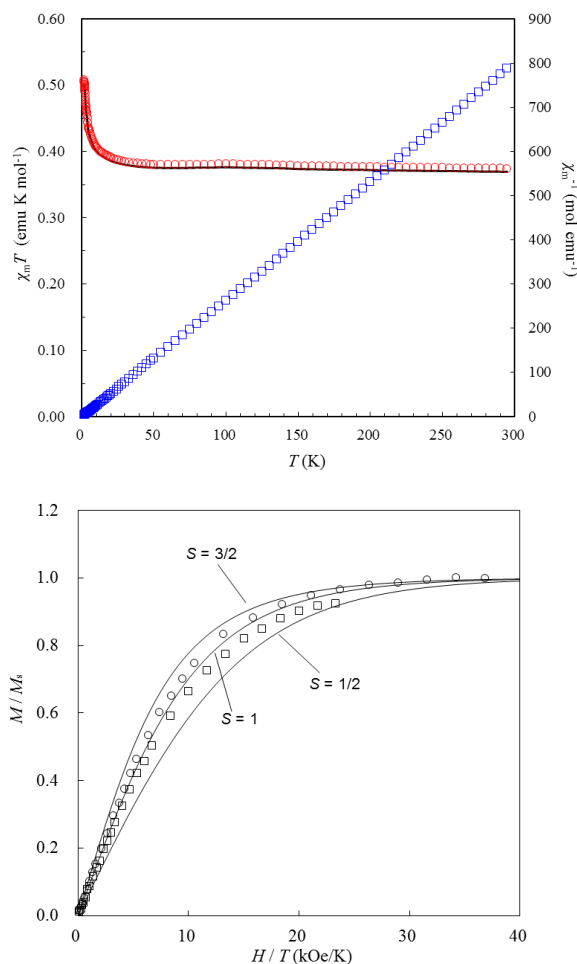


Figure 6 Temperature dependence of χ_m^{-1} (\square) and $\chi_m T$ (\circ) for **2** under the applied field of 5 kOe; the solid line represents the best fit to the Heisenberg 1D chain model (upper). Magnetization isotherm of **2** at 1.9 K (\circ), 3.0 K (\square); the solid lines are the theoretical Brillouin functions for $S = 1/2, 1,$ and $3/2$ (lower).

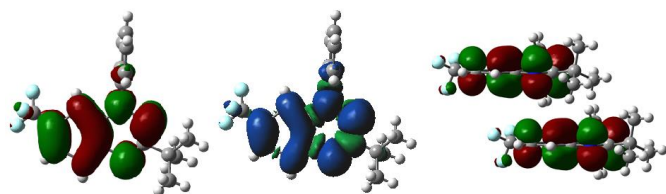


Figure 7 The SOMO(left), spin density(middle) of radical **2** and the overlap of the SOMO in 1D column(right).

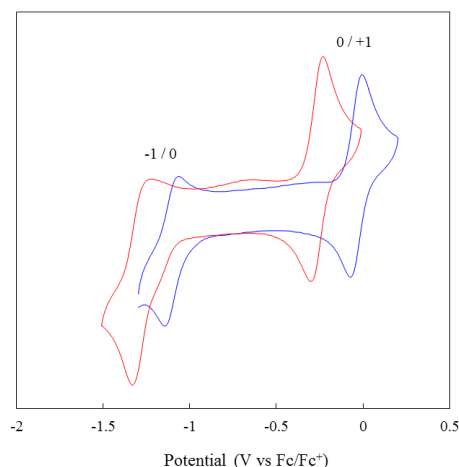


Figure 8 Cyclic voltammograms of **1**(red) and **2**(blue) in CH_3CN containing $n\text{-Bu}_4\text{NPF}_6$ as the electrolyte.

where E and S^2 are the total energy and total spin angular momentum, respectively. The energy gap of the broken symmetry singlet and triplet states was computed at the UB3LYP/6-31G(d) level of theory. The calculated value $J/k_B = +0.6$ K showed that the ferromagnetic interaction was dominant in the column. The overlap of the SOMO is shown in Figure 7. The long distance between the benzotriazinyl moiety leads to a reduced overlap of the SOMO and reduction of the overlap integral and ferromagnetic interaction was exhibited.²⁶ The calculation result was consistent with the magnetic susceptibility measurement.

Cyclic voltammetry and EPR measurement

The cyclic voltammograms of the benzotriazinyl radicals **1** and **2** in CH_3CN are shown in Figure 8. Two reversible waves corresponding to the -1/0 and 0/+1 processes are observed for radicals **1** and **2**. It indicates that the 3-*tert*-butyl benzotriazinyl radical derivatives show a similar redox bistability to Blatter's radical and its analogues. The redox behavior of the derivatives is pseudo reversible due to protonation of the radicals because of trace water.^{13c} The oxidation and reduction potentials of **2** ($E_{0/+1} = -0.040$ V, $E_{-1/0} = -1.11$ V, vs Fc/Fc^+) were higher than those of the parent radical **1** ($E_{0/+1} = -0.27$ V, $E_{-1/0} = -1.29$ V), which show that the electron-withdrawing trifluoromethyl group has an effect on the increase in the oxidation potential and decrease in the energy potential of the SOMO.

The EPR spectra of the benzotriazinyl derivatives in toluene are shown in Figure 9. The spectra exhibit a hyperfine coupling

structure arising from the three non-equivalent nitrogen nuclei in the amidrazonyl ring and hydrogen nuclei in the benzotriazinyl ring and N1-Ph ring. The hyperfine coupling derived from the fluorine nuclei is also observed in the spectra of **2** (Table 1). The assignment of the hyperfine coupling constants (hfccs) are determined according to the ENDOR study of **1** reported by Neugebauer *et al.*¹⁹ The a_{N1} of **2** was slightly higher than that of **1**, however, the a_{N2} and a_{N4} of **2** were slightly lower than those of **1**. This indicates that the substituent effect at 7-position can significantly influence the spin density of N2 and N3.

Table 1 The simulated hfccs and g -factor of radicals **1** and **2**.

Atom	hfcc / G	
	1	2
N1	7.42	7.49
N2	4.86	4.77
N3	5.16	5.06
H3	1.41	1.67
H4	1.07	1.17
H5	1.90	-
H6	0.80	0.72
H9, H13	0.77	0.70
H10, H12	0.52	0.57
H11	0.66	0.65
F	-	3.58
g -factor	2.0039	2.0042

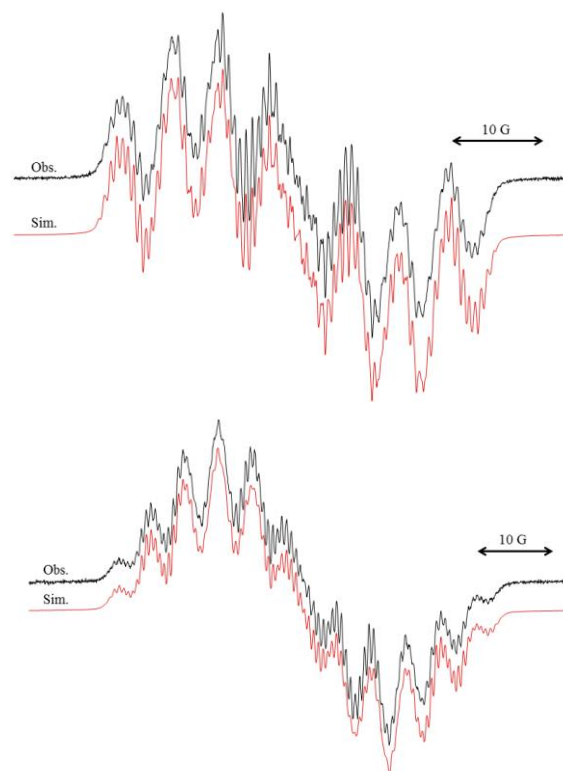
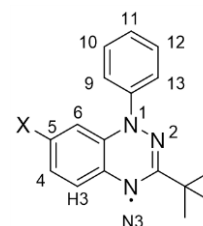


Figure 9 EPR spectra of **1**(upper) and **2**(lower) in toluene at room temperature.

Conclusions

The crystal structure and the magnetic properties of the new benzotriazinyl radical derivative, 3-*tert*-butyl-7-trifluoromethyl-1,4-dihydro-1-phenyl-1,2,4-benzotriazin-4-yl, were investigated.

The radical molecule forms a slipped 1D column structure along the *a* axis. The magnetic susceptibility measurement revealed the existence of an intermolecular ferromagnetic interaction with the magnetic coupling constant $J/k_B = +0.91$ K. The magnetization curve at 1.9 K can be described by the theoretical Brillouin function for the $S = 1$ spin system. The DFT calculation showed that the SOMO was mainly distributed over the benzotriazinyl moiety and trifluoromethyl group. The positive exchange parameter $J/k_B = +0.6$ K predicts the ferromagnetic interaction, which is consistent with the experimental data. The electrochemical study revealed the redox bistability of the 3-*tert*-butyl benzotriazinyl radicals and that the oxidation and reduction potentials of **2** become +0.23 V and +0.18 V higher due to the presence of the trifluoromethyl substituent, respectively. The EPR study showed that spin density was distributed over the molecules that include the substituent. A study of other benzotriazinyl radicals carrying the *tert*-butyl group is now underway.

Experimental section

General information

2-Iodo-4-trifluoromethylaniline²⁷ and *N'*-phenyl-*N*-pivaloylhydrazine (**3**)²⁸ were prepared in the same manner as reported in the literature. The other chemicals were purchased from Wako, TCI Chemicals, Junsei Chemical and Aldrich and used as received. The mass spectroscopy was carried out using a Bruker Ultraflex II (MALDI-TOF, sinapic acid was used as the matrix). The IR spectra were obtained using a JASCO FT/IR-4100. The UV-Vis spectra were recorded in CH₂Cl₂ using a JASCO V-650 spectrophotometer. The crystal data were collected using a Bruker D8 Venture with MoK α (0.71073 Å) radiation. The structures were solved by the direct method using SHELXT-2013²⁹ and refined by F^2 full matrix least squares using SHELXL-2013²⁹ in the Bruker APEX-II program package. The magnetic susceptibility measurement was carried out using a Quantum Design MPMP-XL SQUID magnetometer in the temperature range of 1.8-300 K at 5 kOe. Cyclic voltammograms were recorded in CH₃CN using *n*-Bu₄NPF₆ as the electrolyte. The reference electrode was AgNO₃ and ferrocene was used as the internal reference. The EPR spectra were recorded using a Bruker E500 spectrometer at room temperature. The sample was degassed by the freeze-pump-thaw method. The simulations were carried out using the Winsim2002 program.³⁰

Synthetic procedure

3-*tert*-Butyl-1,4-dihydro-1-phenyl-1,2,4-benzotriazin-4-yl (**1**). The mixture of 2-iodoaniline (219 mg, 1.00 mmol), *N'*-phenyl-*N*-pivaloylhydrazine (250 mg, 1.30 mmol), K₂CO₃ (276 mg, 2.00 mmol) and CuI (19 mg, 0.100 mmol) in dry DMSO (2.5 mL) was heated at 90 °C for 24 h. The reaction mixture was diluted with EtOAc. The organic layer was washed with water, dried over Na₂SO₄ and the solvent was evaporated. The residue was dissolved in AcOH (16 mL) and heated to 100 °C for 10 min. The mixture was cooled to r.t., then aqueous 2M NaOH

was added to make it basic and extracted with CH₂Cl₂ (10 mL). The organic layer was washed with aqueous 2M NaOH \times 2, then the organic layer was separated. To the CH₂Cl₂ solution, aqueous 2M NaOH (10 mL) was added, and the mixture was stirred for 16 h. The organic layer was separated and washed with water, dried over Na₂SO₄ and the solvent was evaporated. The residue was purified by alumina column chromatography (CH₂Cl₂ / *n*-hexane = 1 / 6) and recrystallized from *n*-hexane to give reddish-black crystals. Yield: 91 mg, 34%; LRMS(MALDI-TOF): $m/z = 264$ [M+H]⁺; mp: 106-108 °C; IR(KBr pellet, cm⁻¹): 2957, 2862, 1592, 1580; λ_{\max} (CH₂Cl₂, nm, log ϵ): 241(4.35), 319(3.86), 346(3.82), 426(3.53); Elem. Anal.: Calcd for C₁₇H₁₈N₃: C, 77.24; H, 6.86; N, 15.90. Found: C, 76.98; H, 6.82; N, 15.96; CCDC: 1048595.

3-*tert*-Butyl-7-trifluoromethyl-1,4-dihydro-1-phenyl-1,2,4-benzotriazin-4-yl (**2**). The mixture of 2-iodo-4-trifluoromethylaniline (1.91 g, 6.65 mmol), *N'*-phenyl-*N*-pivaloylhydrazine (1.66 g, 8.65 mmol), K₂CO₃ (1.84 g, 13.3 mmol) and CuI (127 mg, 0.665 mmol) in dry DMSO (16 mL) was heated at 90 °C for 24 h. The reaction mixture was diluted with EtOAc. The organic layer was washed with water, dried over Na₂SO₄ and the solvent was evaporated. The residue was dissolved in AcOH (16 mL) and heated to 100 °C for 10 min. The mixture was cooled to r.t., then aqueous 2M NaOH was added to make it basic and extracted with CH₂Cl₂ (60 mL). The organic layer was washed with aqueous 2M NaOH \times 2, then the organic layer was separated. To the CH₂Cl₂ solution, aqueous 2M NaOH (60 mL) was added, and the mixture was stirred for 16 h. The organic layer was separated and washed with water, dried over Na₂SO₄ and the solvent was evaporated. The residue was purified by alumina column chromatography (CH₂Cl₂ / *n*-hexane = 1 / 6) and recrystallized from CH₃OH to give reddish-black crystals. Yield: 584 mg, 26%; LRMS(MALDI-TOF): $m/z = 333$ [M+H]⁺; mp: 86-88 °C; IR(KBr pellet, cm⁻¹): 2973, 2868, 1593, 1270; λ_{\max} (CH₂Cl₂, nm, log ϵ): 242(4.43), 259(4.18), 319(3.93), 343(3.80), 432(3.58); Elem. Anal.: Calcd for C₁₈H₁₇F₃N₃: C, 65.05; H, 5.16; F, 17.15; N, 12.64. Found: C, 65.04; H, 5.12; F, 17.1; N, 12.53; CCDC: 1048596.

Acknowledgements

This work was partly supported by a Grant-in-Aid for Scientific Research (No. 25620066) from MEXT, Japan and the MEXT-Supported Program for the Strategic Research Foundation at Private Universities, 2012-2016.

Notes and references

yoshioka@applc.keio.ac.jp

Department of Applied Chemistry, Faculty of Science and Technology, Keio University, Yokohama 223-8522, Japan

Electronic Supplementary Information (ESI) available: [UV-Vis spectra, crystallographic data and DFT output data]. See DOI: 10.1039/b000000x/

- (a) *Magnetic Properties of Organic Materials*, ed. P. M. Lahti, Marcel Dekker: New York, 1999. (b) *Stable Radicals: Fundamentals*

- and Applied Aspects of Odd-Electron Compounds; ed. R. G. Hicks, Wiley: Chichester, U.K., 2010. (c) *Encyclopedia of Radicals in Chemistry, Biology and Materials*, ed. C. Chatgililoglu and A. Studer, Hoboken, NJ, Wiley, 2012.
- 2 (a) O. H. Griffith and A. S. Waggoner, *Acc. Chem. Res.* 1969, **2**, 17. (b) C. S. Klug and J. B. Feix, *Methods Cell Biol.* 2008, **84**, 617. (c) Q. Z. Ni, E. Daviso, T. V. Can, E. Markhasin, A. K. Jawla, T. M. Swager, R. J. Temkin, J. Herzfeld and R. G. Griffin, *Acc. Chem. Res.* 2013, **46**, 1933.
- 3 (a) Z. Zhang, P. Chen, T. N. Murakami, S. M. Zakeerddin and M. Gratzel, *Adv. Funct. Mater.* 2008, **18**, 341. (b) R. Y.-Y. Lin, T.-C. Chu, P.-W. Chen, J.-S. Ni, P.-C. Sih, Y.-C. Chen, K.-C. Ho and J. T. Lin, *ChemSusChem* 2014, **7**, 2221.
- 4 (a) Y. Morita, S. Nishida, T. Murata, M. Moriguchi, A. Ueda, M. Satoh, K. Arifuku, K. Sato and T. Takui, *Nat. Mater.* 2011, **10**, 947. (b) A. Sarkar, M. E. Itkis, F. S. Tham and R. C. Haddon, *Chem. Eur. J.* 2011, **17**, 11576. (c) Y. Miura, H. Chiba, R. Katoono, H. Kawai, K. Fujiwara, S. Suzuki, K. Okada and T. Suzuki, *Tetrahedron Lett.* 2012, **53**, 6561. (d) A. Mailman, S. M. Winter, X. Yu, C. M. Robertson, W. Yong, J. S. Tse, R. A. Secco, Z. Liu, P. A. Dube, J. A. K. Howard and R. T. Oakley, *J. Am. Chem. Soc.* 2012, **134**, 9886.
- 5 (a) M. Kinoshita, *Jpn. J. Appl. Phys.* 1994, **33**, 5718. (b) H. Iwamura, *Polyhedron* 2013, **66**, 3.
- 6 M. Tamura, Y. Nakazawa, D. Shiomi, K. Nozawa, Y. Hosokoshi, M. Ishikawa, M. Takahashi and M. Kinoshita, *Chem. Phys. Lett.* 1991, **186**, 401.
- 7 (a) P. M. Allemand, G. Srdanov and F. Wudl, *J. Am. Chem. Soc.* 1990, **112**, 9391. (b) M. Yao, S. Asakura, M. Abe, H. Inoue and N. Yoshioka, *Cryst. Growth Des.* 2005, **5**, 413. (c) M. Yao, H. Inoue and N. Yoshioka, *Chem. Phys. Lett.* 2005, **402**, 11.
- 8 Y. Hosokoshi, M. Tamura, M. Kinoshita, H. Sawa, R. Kato, Y. Fujiwara and Y. Ueda, *J. Mater. Chem.* 1994, **4**, 1219.
- 9 K. Nozawa, Y. Hosokoshi, D. Shiomi, M. Tamura, N. Iwasawa, H. Sawa, R. Kato and M. Kinoshita, *Synth. Met.* 1993, **55-57**, 3323.
- 10 M. Deumal, J. M. Rawson, A. E. Goeta, J. A. K. Howard, R. C. B. Copley, M. A. Robb and J. J. Novoa, *Chem. Eur. J.* 2010, **16**, 2741.
- 11 H. M. Blatter and H. Lukaszewski, *Tetrahedron Lett.* 1968, **9**, 2701.
- 12 (a) P. A. Koutentis and D. Lo Re, *Synthesis* 2010, **12**, 2075. (b) A. A. Berezin, G. Zissimou, C. P. Constantinides, Y. Beldjoudi, J. M. Rawson and P. A. Koutentis, *J. Org. Chem.* 2014, **79**, 314.
- 13 (a) C. P. Constantinides, P. A. Koutentis and J. M. Rawson, *Chem. Eur. J.* 2012, **18**, 15443. (b) C. P. Constantinides, E. Carter, D. M. Murphy, M. Manoli, G. M. Leitus, M. Bendicov, J. M. Rawson and P. A. Koutentis, *Chem. Commun.* 2013, **49**, 8662. (c) A. A. Berezin, C. P. Constantinides, S. I. Mirallai, M. Manoli, L. L. Cao, J. M. Rawson and P. A. Koutentis, *Org. Biomol. Chem.* 2013, **11**, 6780. (d) C. P. Constantinides, A. A. Berezin, M. Manoli, G. M. Leitus, G. A. Zissimou, M. Bendikov, J. M. Rawson and P. A. Koutentis, *Chem. Eur. J.* 2014, **20**, 5388. (e) C. P. Constantinides, A. A. Berezin, M. Manoli, G. M. Leitus, G. A. Zissimou, M. Bendikov, J. M. Rawson and P. A. Koutentis, *New J. Chem.* 2014, **38**, 949. (f) I. S. Morgan, A. Peuronen, M. M. Hanninen, R. W. Reed, R. Clerac and H. M. Ruononen, *Inorg. Chem.* 2014, **53**, 33.
- 14 M. Fumanal, S. Vela, J. Ribas-ariño and J. J. Novoa, *Chem. Asian J.* 2014, **9**, 3612.
- 15 (a) C. P. Constantinides, P. A. Koutentis and G. Loizou, *Org. Biomol. Chem.* 2011, **9**, 3122. (b) Y. Takahashi, Y. Miura and N. Yoshioka, *Chem. Lett.* 2014, **43**, 1236. (c) A. Bodzioch, M. Zheng, P. Kaszynski and G. Utecht, *J. Org. Chem.* 2014, **79**, 7294.
- 16 (a) B. Yan, J. Cramen, R. McDonald and N. L. Frank, *Chem. Commun.* 2011, **47**, 3201. (b) C. P. Constantinides, P. A. Koutentis and J. M. Rawson, *Chem. Eur. J.* 2012, **18**, 7109.
- 17 C. P. Constantinides, P. A. Koutentis, H. Krassos, J. M. Rawson and A. J. Tasiopoulos, *J. Org. Chem.* 2011, **76**, 2798.
- 18 C. P. Constantinides, A. A. Berezin, G. A. Zissimou, M. Manoli, G. M. Leitus, M. Bendikov, M. R. Probert, J. M. Rawson and P. A. Koutentis, *J. Am. Chem. Soc.* 2014, **136**, 11906.
- 19 F. A. Neugebauer and G. Rimmler, *Magn. Reson. Chem.* 1988, **26**, 595.
- 20 K. Mukai, K. Inoue, N. Achiwa, J. B. Jamali, C. Krieger and F. A. Neugebauer, *Chem. Phys. Lett.* 1994, **224**, 569.
- 21 X. Xiong, Y. Jiang and D. Ma, *Org. Lett.* 2012, **14**, 2552.
- 22 A. T. Gubaidullin, B. I. Buzykin, I. A. Litvinov and N. G. Gazetdinova, *Russ. J. Gen. Chem.* 2004, **74**, 939.
- 23 G. A. Baker Jr., G. S. Rushbrooke and H. E. Gilbert, *Phys. Rev. A* 1964, **135**, 1272.
- 24 M. J. Frisch, G. W. Trucks, H. B. Schlegel, G. E. Scuseria, M. A. Robb, J. R. Cheeseman, J. A. Montgomery, Jr., T. Vreven, K. N. Kudin, J. C. Burant, J. M. Millam, S. S. Iyengar, J. Tomasi, V. Barone, B. Mennucci, M. Cossi, G. Scalmani, N. Rega, G. A. Petersson, H. Nakatsuji, M. Hada, M. Ehara, K. Toyota, R. Fukuda, J. Hasegawa, M. Ishida, T. Nakajima, Y. Honda, O. Kitao, H. Nakai, M. Klene, X. Li, J. E. Knox, H. P. Hratchian, J. B. Cross, C. Adamo, J. Jaramillo, R. Gomperts, R. E. Stratmann, O. Yazyev, A. J. Austin, R. Cammi, C. Pomelli, J. W. Ochterski, P. Y. Ayala, K. Morokuma, G. A. Voth, P. Salvador, J. J. Dannenberg, V. G. Zakrzewski, S. Dapprich, A. D. Daniels, M. C. Strain, O. Farkas, D. K. Malick, A. D. Rabuck, K. Raghavachari, J. B. Foresman, J. V. Ortiz, Q. Cui, A. G. Baboul, S. Clifford, J. Cioslowski, B. B. Stefanov, G. Liu, A. Liashenko, P. Piskorz, I. Komaromi, R. L. Martin, D. J. Fox, T. Keith, M. A. Al-Laham, C. Y. Peng, A. Nanayakkara, M. Challacombe, P. M. W. Gill, B. Johnson, W. Chen, M. W. Wong, C. Gonzalez and J. A. Pople, *Gaussian03 (Revision B.04)*, Gaussian, Inc., Pittsburgh PA, 2003.
- 25 K. Yamaguchi, H. Fukui and T. Fueno, *Chem. Lett.* 1986, **15**, 625.
- 26 The distance between the benzotriazinyl rings is too long to form π - π interaction, however, the magnetic interaction was observed in galvinoxyl with ca. 4 Å separation.³¹
- 27 J. Iskra, S. Stavber and M. Zupan, *Synthesis* 2004, **11**, 1869.
- 28 G. Kaugers and C. Mich, US patent 3,870,505, Mar. 11, 1975.
- 29 G. M. Sheldrick, *Acta. Cryst.* 2008, **A64**, 112.
- 30 D. A. O'Brien, D. R. Duling and Y. C. Fann, Public EPR Software Tools: *Winsim Spectral Simulation for MS- Windows 9x, NT v0.98*, NIEHS, National Institute of Health, Bethesda, MD.
- 31 (a) N. Azuma, J. Yamauchi, K. Mukai, H. Ohya-Nishiguchi and Y. Deguchi, *Bull. Chem. Soc. Jpn.* 1973, **46**, 2728. (b) F. Dietz, N. Tyutyulkov and M. Baumgarten, *J. Phys. Chem. B* 1998, **102**, 3912.